



# Efficacy of core biopsies for diagnosing inflammatory myofibroblastic tumors in pediatric patients: case series from a single tertiary referral center

Ugo Maria Pierucci<sup>1</sup>, Irene Paraboschi<sup>2</sup>, Carlotta Ardenghi<sup>1</sup>, Camilla Viglio<sup>1</sup>,  
Giorgio Giuseppe Orlando Selvaggio<sup>1</sup>, Giulia Lanfranchi<sup>1</sup>, Michela Casanova<sup>3</sup>, Paola Collini<sup>4</sup>,  
Marta Barisella<sup>5</sup>, Marcello Napolitano<sup>6</sup>, Anna Camporesi<sup>7</sup>, Gloria Pelizzo<sup>1,2</sup>

<sup>1</sup>Department of Pediatric Surgery, “V. Buzzi” Children’s Hospital, Milan, Italy; <sup>2</sup>Department of Biomedical and Clinical Sciences, University of Milan, Milan, Italy; <sup>3</sup>Pediatric Oncology Unit, Medical Oncology Department, Fondazione IRCCS Istituto Nazionale Tumori, Milan, Italy; <sup>4</sup>Department of Pathology and Laboratory Medicine, Fondazione IRCCS Istituto Nazionale Tumori, Milan, Italy; <sup>5</sup>Pathology Unit, ASST Fatebenefratelli Sacco, Milan, Italy; <sup>6</sup>Department of Pediatric Radiology and Neuroradiology, “V. Buzzi” Children’s Hospital, Milan, Italy; <sup>7</sup>Pediatric Anesthesia and Intensive Care Unit, “V. Buzzi” Children’s Hospital, Milan, Italy

*Contributions:* (I) Conception and design: UM Pierucci, I Paraboschi, G Pelizzo; (II) Administrative support: C Ardenghi, C Viglio, GGO Selvaggio, M Napolitano, A Camporesi; (III) Provision of study materials or patients: G Ardenghi, G Lanfranchi, M Casanova, P Collini, M Barisella, M Napolitano, A Camporesi; (IV) Collection and assembly of data: UM Pierucci, I Paraboschi; (V) Data analysis and interpretation: UM Pierucci, I Paraboschi, G Pelizzo, P Collini, M Barisella; (VI) Manuscript writing: All authors; (VII) Final approval of manuscript: All authors.

*Correspondence to:* Gloria Pelizzo, MD. Department of Biomedical and Clinical Sciences, University of Milan Via Giovanni Battista Grassi 74, 20157 Milan, Italy; Department of Pediatric Surgery, “V. Buzzi” Children’s Hospital Via Lodovico Castelvetro, 32, 20154 Milan, Italy. Email: gloria.pelizzo@unimi.it.

**Background:** Inflammatory myofibroblastic tumors (IMTs) are rare, often non-metastasizing neoplasms characterized by fibro/myofibroblastic spindle cells with varying infiltrates of plasma cells, lymphocytes, and/or eosinophils. Despite their generally indolent nature, IMTs can exhibit locally aggressive behavior and a significant tendency for local recurrence, making complete surgical resection the standard treatment approach. Accurate diagnosis can be challenging due to the overlap in imaging features with more aggressive tumors, necessitating preoperative biopsies to enable differential diagnosis and guide treatment decisions. The complexity of distinguishing IMTs from other malignancies underscores the importance of biopsy in establishing an accurate diagnosis and planning appropriate management strategies.

**Case Description:** This study presents the cases of four pediatric patients (three males, one female) diagnosed with IMT, involving tumors located in the lung (one case), bladder (one case), and liver (two cases). Initial minimally invasive biopsies, including a US-guided tru-cut core biopsy and a percutaneous core biopsy in one case, as well as endoscopic core biopsies in two other cases, yielded inconclusive results. These initial procedures failed to provide definitive diagnostic information, necessitating the use of more precise diagnostic techniques to achieve a definitive histological diagnosis of IMT.

**Conclusions:** The findings indicate that when initial biopsy results are inconclusive in cases suspected to be IMT, more precise diagnostic procedures may be necessary to secure a definitive diagnosis. This highlights the need for careful consideration of alternative biopsy methods to ensure accurate identification and effective management of IMT in pediatric patients.

**Keywords:** Inflammatory myofibroblastic tumor (IMT); pediatric; neoplasms; core biopsy; case series

Submitted Jun 20, 2024. Accepted for publication Sep 04, 2024. Published online Oct 28, 2024.

doi: 10.21037/tp-24-239

View this article at: <https://dx.doi.org/10.21037/tp-24-239>

## Introduction

Inflammatory myofibroblastic tumors (IMTs) are uncommon visceral and soft-tissue neoplasms occurring in children and young adults (1,2). These tumors can develop in various anatomical locations, although they most commonly occur in the abdominal soft tissues (mesentery, omentum, retroperitoneum, pelvis), lung, mediastinum, head and neck, gastrointestinal tract, and genitourinary tract. Unusual locations include the liver, limbs, and central nervous system (3).

The exact cause of IMT remains uncertain, as some cases are associated with infectious or inflammatory conditions, while others appear to arise spontaneously without a clear underlying cause (4–6). Most IMTs are rarely metastasizing lesions, although a subset are malignant (4–6). Given their low frequency, long-term follow-up of IMT is scarcely reported in the scientific literature. However, anecdotal cases of long-term remission have been described when radical tumor excision is achieved (7).

Diagnosis of IMTs can be challenging due to their heterogeneous histologic appearance, characterized by variable cellularity of fibro/myofibroblastic spindle cells intermixed with an inflammatory infiltrate consisting of plasma cells, lymphocytes, and eosinophils (8). IMT exhibits distinct somatic characteristics in approximately

50–60% of cases (2,9). A specific molecular feature is associated with these neoplasms: it is the rearrangement of the anaplastic lymphoma kinase (ALK) gene, which encodes a receptor tyrosine kinase (2,9). These rearrangements lead to fusion with various gene partners, producing a persistently activated protein that can be detected through immunohistochemistry (IHC). Additionally, other kinase gene fusions are present in smaller subsets of IMT cases, including ROS1 (around 10% of cases) and NTRK3 among the most frequent (2,9). Finding these targets plays a potential therapeutic role and it can be detected primarily by IHC, and then by fluorescence in situ hybridization (FISH), and next-generation sequencing (NGS). Molecular determination has therefore become essential in these neoplasms (2,9).

While core biopsies are typically sufficient for definitively diagnosing most solid tumors in pediatric patients, our study describes 4 cases of IMT where they yielded inconclusive results. In these instances, more precise procedures were necessary to achieve an accurate diagnosis and initiate targeted interventions with tyrosine kinase inhibitors, whether appropriate. We present this article in accordance with the AME Case Series reporting checklist (available at <https://tp.amegroups.com/article/view/10.21037/tp-24-239/rc>).

## Case presentation

All consecutive cases of IMT diagnosed in our academic pediatric tertiary referral center, the “Vittore Buzzi” Children’s Hospital, where core biopsies yielded inconclusive results, were described.

All procedures performed in this study were in accordance with the ethical standards of the institutional and/or national research committee(s) and with the Helsinki Declaration (as revised in 2013). According to our Institution’s regulations (Department of Pediatric Surgery, Children’s Hospital “Vittore Buzzi”, Milan, Italy), the need for ethical approval for this non-interventional study’s retrospectively obtained and anonymized data was waived. The reservedness of the collected information was ensured according to Regulation (EU)/2016/679 GDPR [Regulation (EU) 2016/679], Legislative Decree n.101/18. Full informed consent was obtained from the study participants’ guardians.

### Case 1

A 3-year-old boy was brought to our pediatric tertiary

### Highlight box

#### Key findings

- When dealing with inflammatory myofibroblastic tumors (IMTs) advanced biopsy techniques are needed to provide a definitive diagnosis, ensuring accurate identification and appropriate management of IMT.

#### What is known and what is new?

- IMTs are rare, locally aggressive neoplasms with a risk of recurrence, requiring complete surgical resection for effective treatment. Radiographic imaging alone often fails to distinguish IMT from other aggressive tumors, making preoperative biopsies essential for accurate diagnosis.
- More precise diagnostic procedures are required to obtain a definitive histological diagnosis when initial biopsies are non-diagnostic, highlighting the limitations of standard biopsy techniques in effectively identifying IMT.

#### What is the implication, and what should change now?

- Minimally invasive biopsies often fail in diagnosing IMT. To address this, there is a need for enhanced diagnostic protocols and the adoption of more precise biopsy techniques when initial results are non-diagnostic.



**Figure 1** Case 1. (A) CXR revealing a radiopacity near the right lower para-cardiac area (\*) along with diffuse thickening of the peribronchovascular interstitium. (B) Lung US scan confirming an extensive parenchymal consolidation in the RLL, characterized by coarse areas of inhomogeneous echotexture and hyperechogenic spots within lobulated profiles. (C,D) Chest CT scan showing a solid lesion in the RLL measuring 6 cm × 6 cm × 5 cm, with some millimetric calcifications (\*). The mass appeared inseparable from adjacent structures, including the hemidiaphragm, chest wall, hilum of the right lung, thoracic esophagus, and aorta. Additionally, involvement of the left atrium and right superior pulmonary vein, as well as the right middle and inferior lobar bronchi, was noted. CXR, chest X-ray; US, ultrasound; RLL, right lower lobe; CT, computed tomography.

referral center with a persistent dry, hacking cough that had not responded to typical treatments for upper respiratory tract infections. Complete blood count (CBC) tests showed findings consistent with hypochromic microcytic anemia (hemoglobin 78 g/L, MCV 58.1 fL), mild thrombocytosis (platelet count  $568 \times 10^9/L$ ), and elevated inflammatory markers (white blood cell count  $7.99 \times 10^9/L$ , CRP 96.2 mg/L). The chest X-ray (CXR) revealed a radiopacity in the right lower para-cardiac region, accompanied by diffuse thickening of the peribronchovascular interstitium (Figure 1A). The respiratory pathogens panel test returned negative results, and serum tumor markers, including  $\alpha$ -fetoprotein, carcinoembryonic antigen, neuron-specific

enolase, and human chorionic gonadotropin, were all within normal ranges.

On the lung ultrasound (US) scan, a parenchymal consolidation was observed in the right lower lobe (RLL), characterized by coarse areas of inhomogeneous echotexture and hyperechogenic spots within lobulated profiles (Figure 1B). The chest computed tomography (CT) scan revealed a solid lesion measuring 6 cm × 6 cm × 5 cm in size located in the RLL. The lesion exhibited some millimetric calcifications. Importantly, it did not present a frank cleavage plane from adjacent structures, including the right hemidiaphragm, ipsilateral chest wall, right lung hilum, thoracic esophagus, and the aorta. Additionally, the

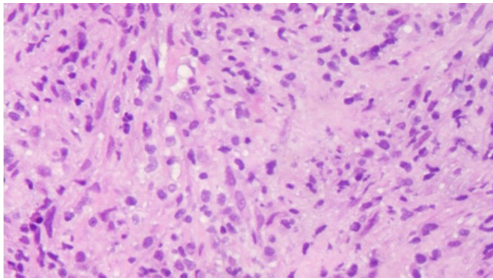


**Figure 2** Case 1. 40× hematoxylin and eosin-stained specimen of the CT-guided core needle biopsy showing a proliferation of short spindle cells of myofibroblastic type without significant cytological atypia, growing in a collagenic stroma with a conspicuous inflammatory component of lymphocytes and plasma cells. Subsequent genetic analysis using NGS identified a fusion between TFG (exon 4) and ROS1 (exon 35). CT, computed tomography; NGS, next-generation sequencing.

lesion was noted to have an impression on the left atrium and the right superior pulmonary vein, both displaying irregular and potentially infiltrated profiles. Furthermore, the right middle and inferior lobar bronchi appeared to be involved, as depicted in *Figure 1C,1D*. Given the substantial size of the mass and its infiltration into adjacent thoracic structures, radical excision was deemed unfeasible. Consequently, following a multidisciplinary team meeting, a US-guided 18G tru-cut core needle biopsy was performed. Unfortunately, the histopathological examination of this biopsy yielded inconclusive results for a definitive diagnosis. The same procedure was then repeated using a US-guided 18G tru-cut core needle. Once again, the results were inconclusive. The biopsy showed a proliferation of short spindle cells of myofibroblastic type without significant cytological atypia, with a conspicuous inflammatory component of lymphocytes and plasma cells and a solid inter- and intra-alveolar growth. These results were however inclusive of a definitive diagnosis of IMT (*Figure 2*). Subsequently, a CT-guided core needle biopsy was performed. Finally, the histopathological examination of this third specimen revealed a myofibroblastic proliferation with a low inflammatory component, consistent with a final diagnosis of IMT. FISH testing revealed no ALK rearrangements. Molecular analysis using NGS identified a fusion between the TFG gene (exon 4) and the ROS1 gene (exon 35) at a low frequency. This fusion is characteristic of a minority of IMT (10). Following the initiation of a weekly regimen of Vinorelbine and Methotrexate, a 2-month follow-up CT scan showed no significant reduction in

the size of the thoracic mass. Consequently, the initial chemotherapy regimen was discontinued, targeted therapy was successfully commenced and the patient was finally operated on.

### Case 2

A 15-year-old boy with a history of lower urinary tract symptoms, including suprapubic pain associated with dysuria and strangury, underwent comprehensive testing, including CBC, dipstick urinalysis, and urine culture tests. All results returned within normal limits. Following the suspicion of an infectious urinary abscess, raised by an abdominal CT scan (which revealed a thickened bladder wall, particularly on the right side), further investigations were pursued (*Figure 3A,3B*). Immunological tests for human schistosomiasis and fecal parasitological tests returned negative results. Consequently, the patient was referred to our pediatric tertiary referral center, where a US scan of the urinary tract (*Figure 3C*) and a diagnostic cystoscopy were performed. The endoscopic examination revealed diffuse bladder inflammation and ectasia of the vascular network, consistent with eosinophilic cystitis. Core biopsies of the bladder lesion were obtained using an endoscopic gripper device during the procedure. Following the endoscopic evaluation, the patient was discharged with painkillers and oxybutynin treatments, along with instructions for a follow-up bladder US scan (*Figure 3D*). Despite the histopathological analysis yielding inconclusive results, the report was negative for malignancy or infectious disease. As the bladder lesion persisted without signs of spontaneous resolution on the follow-up urinary tract US scan, a decision was made to proceed with an open extravesical radical surgical excision. During the surgical procedure, the bladder lesion was observed to be greyish and solid upon palpation, measuring 3.4 cm × 2.5 cm × 2.2 cm in size. The histopathological analysis showed a rich proliferation of spindle cells growing in an infiltrative manner with occasional atypical elements, but inconsistent mitotic index, and focal areas of necrosis (probably due to the previous endoscopic procedure), providing a final diagnosis of IMT (*Figure 4*). The fluorescence in situ hybridization (FISH) analysis revealed a rearrangement of the ALK gene, further supporting the diagnosis. Considering the favorable outcome and absence of residual disease, no adjuvant treatment was deemed necessary. During the last follow-up visit 3 years after surgery, the patient was found to be in good health and free from urinary symptoms. The follow-up urinary tract US scan revealed no signs of residual neoplasia

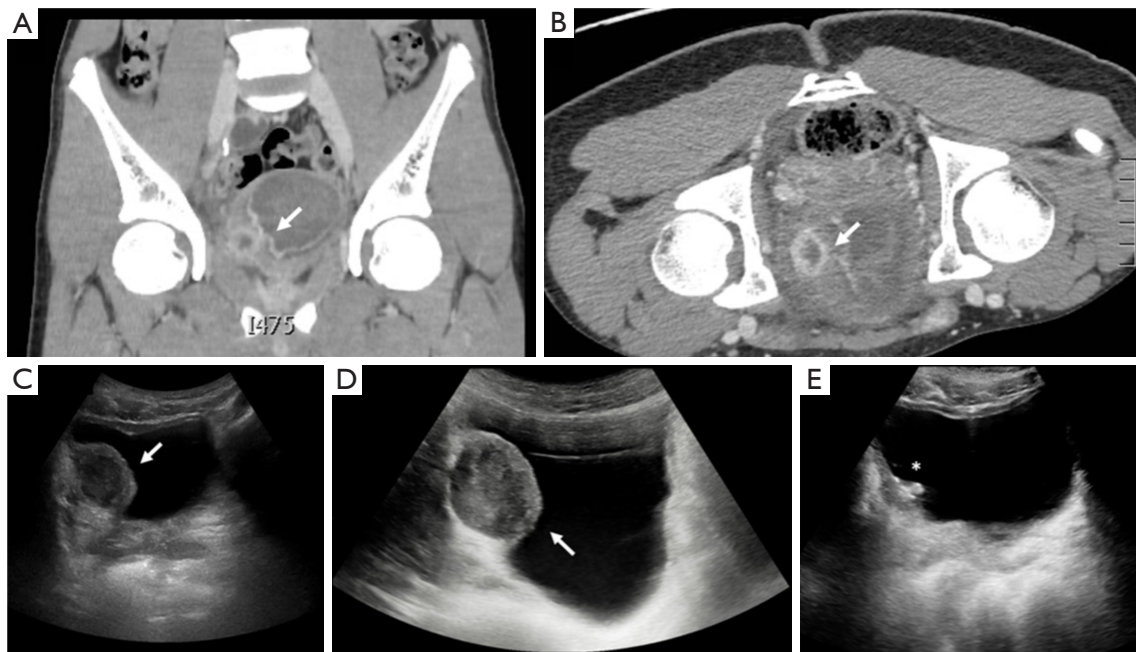


**Figure 3** Case 2. A coronal (A) and transverse (B) abdominal CT scans showing a thickening of the bladder wall, predominantly on the right side. Preoperative (C,D) and postoperative (E) US scans depicting a 3.4 cm × 2.5 cm × 2.2 cm rounded lesion with sharp and well-defined margins, exhibiting inhomogeneous hypoechoic echostructure involving the right lateral bladder wall. The lesion is indicated before (→) and after (\*) the radical open extravesical complete surgical excision. CT, computed tomography; US, ultrasound.

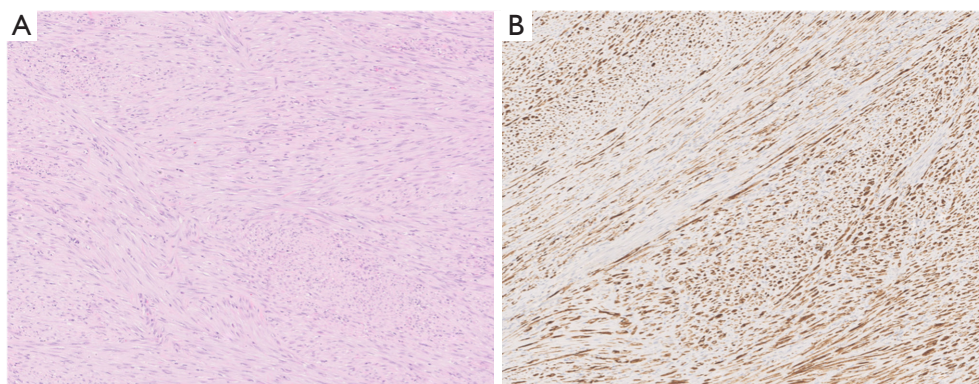


**Figure 4** Case 2. 10× hematoxylin and eosin (A) and ALK immunohistochemical (B) stained specimen of the lesion revealing a hypercellular proliferation of spindle cells in short fascicles with occasional atypical elements but inconsistent mitotic index. The final diagnosis of IMT of the bladder was reached. FISH analysis indicated the presence of ALK gene translocation. ALK, anaplastic lymphoma kinase; IMT, inflammatory myofibroblastic tumor; FISH, fluorescence in situ hybridization.

(Figure 3E).

### Case 3

An 8-year-old boy presented at our pediatric tertiary referral center with complaints of persistent pain in the

right hypochondrium and significant weight loss (2 kg in the last month). His medical history included acholic stools and hyperchromic urine, which had appeared 2 weeks prior. Upon physical examination, signs of jaundice were observed, with abdominal tenderness noted upon palpation of the right quadrants. The liver margins were palpable 1–2 cm below

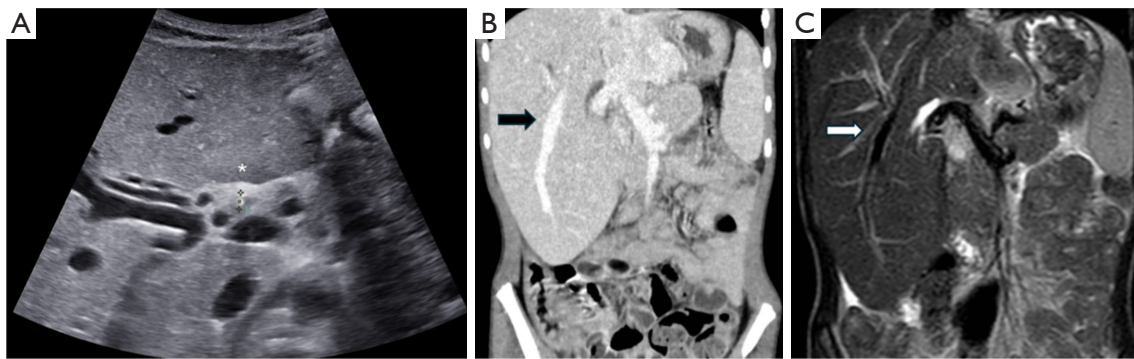


**Figure 5** Case 3. Abdominal US scan (A), contrast-enhanced chest and abdominal CT scan (B), and cholangiography-MRI (C) revealing an altered structure of the left hepatic lobe (\*), along with a diffuse dilatation of the bile ducts (→), which appeared to be centrally dislocated. CT, computed tomography; US, ultrasound; MRI, magnetic resonance imaging.

the costal arch and of firm consistency. Blood tests revealed elevated inflammatory markers (white blood cell count:  $13.34 \times 10^9/L$ ; C-reactive protein: 18.9 mg/L; procalcitonin: 1.7 mcg/L) and elevated levels of IgG4 immunoglobulin subtypes [IgG: 18.23 g/L (normal range: 4.63–12.8 g/L), IgG4 2,957 mg/L (normal range: 40–865 mg/L)]. Liver function tests (LFT) showed elevated levels of bilirubin (direct bilirubin: 5.61 mg/dL; indirect bilirubin: 2.29 mg/dL); transaminases [aspartate aminotransferase (AST): 288 U/L; alanine aminotransferase (ALT): 220 U/L],  $\gamma$ -glutamyl transferase ( $\gamma$ GT: 684 U/L), and alkaline phosphatase (1,012 U/L). Virological and tumor marker tests yielded negative results. Regarding imaging studies, the abdominal US scan revealed an altered structure of the left hepatic lobe and diffuse dilatation of the bile ducts, which appeared to be centrally dislocated (*Figure 5A*). The contrast-enhanced chest and abdominal CT scan confirmed liver enlargement, measuring 16 cm in lateral diameter, with the inferior margins reaching the right upper iliac crest. A space-occupying mass in the left hepatic lobe was identified, infiltrating the hepatic hilum and biliary carrefour, causing significant dilatation of the biliary tract (*Figure 5B*). Subsequent magnetic resonance imaging cholangiography was performed, revealing a lesion with a grossly oval morphology measuring 30 cm  $\times$  35 cm. The lesion displayed an inhomogeneous signal, predominantly modestly hyperintense in T2 and hypointense in T1 compared to normal liver parenchyma, with evidence of diffusivity restriction (*Figure 5C*). These findings raised suspicion for either an IMT of the liver, IgG4 autoimmune cholangitis, or rarer hepatic pediatric tumors. Aiming to further characterize the nature of the lesion, an endoscopic procedure was scheduled. Under endoscopic US guidance,

the right bile duct was punctured, and multiple core biopsies of the lesion were obtained using an endoscopic gripper. Subsequently, a 12-Ch stent was placed in the right bile duct. The left bile duct was also punctured under US guidance, and an 8-Ch internal-external biliary drain was inserted. Following the procedure, the patient's symptoms improved, and there was a significant decrease in total and direct bilirubin levels (total bilirubin 2.82 mg/dL, direct bilirubin 2.12 mg/dL, indirect bilirubin 0.7 mg/dL). However, the results of the endoscopic core biopsies of the hepatic lesion were inconclusive. The hepatic parenchyma showed its typical architecture with slightly enlarged portal spaces due to mild edema associated with mild periductal granulocytic inflammation, with the presence of rare lymphocytes (mostly T cells) and isolated eosinophils. No morphological or immunocytochemical evidence of plasma cells was observed. Therefore, in the need to reach a definite diagnosis, the patient underwent a scheduled open biopsy performed under US guidance. The final diagnosis was IMT associated with the rearrangement of the ROS1 gene (see *Figure 6*). Subsequently, under cholangiography guidance, the external-internal drainage was replaced with an internal biliary stent, and the patient was safely discharged home. The patient received 10 weekly chemotherapy doses of vinorelbine and methotrexate and then targeted therapy for insufficient response, which is still ongoing.

#### Case 4

A 4-year-old girl presented at our pediatric tertiary referral center complaining of gastrointestinal symptoms (i.e., vomiting and diarrhea) associated with cholestatic jaundice,

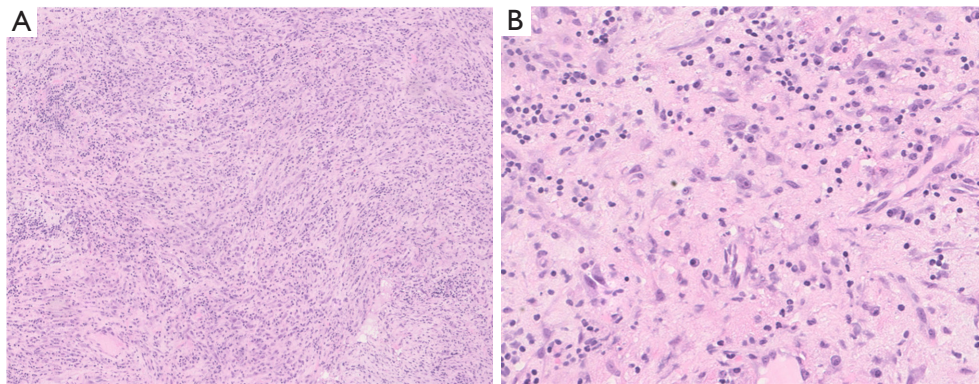


**Figure 6** Case 3. 10× (A) and 40× (B) hematoxylin and eosin stained specimen obtained from an open biopsy performed under US guidance showing a proliferation of spindle and epithelioid ganglion-like cells with eosinophilic cytoplasm and prominent nucleoli of myofibroblastic type in collagenic stroma, intermixed with lymphocytes, plasma cells, and eosinophils. The final diagnosis of IMT was provided. FISH analysis indicated a rearrangement of the ROS1 gene. US, ultrasound; IMT, inflammatory myofibroblastic tumor; FISH, fluorescence in situ hybridization.



**Figure 7** Case 4. Abdominal US scan (A), MRI (B), and contrast-enhanced CT scan (C), showing the lesion of the right hepatic lobe (\* in A and C; → in B) with a diffusely infiltrative appearance and poorly defined margins. US, ultrasound; MRI, magnetic resonance imaging; CT, computed tomography.

clay-colored feces, and itching. Upon admission, on physical examination, the liver was palpable at the costal arch. LFT showed elevated levels of bilirubin (direct bilirubin: 5.46 mg/dL; indirect bilirubin: 1.98 mg/dL), transaminases (AST: 256 U/L; ALT: 328 U/L),  $\gamma$ GT (367 U/L), and alkaline phosphatase (1,312 U/L). Virological and tumor marker tests yielded negative results. An abdominal US scan was performed, showing a heterogeneous alteration at the level of the VIII segment with poorly defined margins and a maximum diameter of approximately 5 cm, extending almost to the hilum, causing dilation of the intrahepatic bile ducts (*Figure 7A*). The abdominal MRI showed the presence of extensive signal alteration in the liver, predominantly in the right lobe at segments 5 and 8, with poorly defined margins [diameters of approximately 48 mm  $\times$  37 mm  $\times$  35 mm;

lateral length (LL)  $\times$  anteroposterior dimension (AP)  $\times$  cranio-caudal dimension (CC)]. This lesion appeared heterogeneous, with a faintly hyperintense signal on T2-weighted imaging and a hypointense signal on T1-weighted imaging compared to the surrounding hepatic parenchyma, without a clear signal restriction on diffusion-weighted imaging/apparent diffusion coefficient (DWI/ADC). After contrast agent administration, a heterogeneous enhancement was observed except in the ultra-late phases (after nearly an hour and a half), where the lesion appeared heterogeneously hypointense compared to the remaining hepatic parenchyma. The arterial vascular branches were directed toward the signal alteration and the hepatic artery appeared more prominent than usual. This alteration seemed to extend peripherally in a subcapsular location up to the region of the hepatic hilum, with apparent compression

on some bile duct branches, accompanied by significant dilation of the intrahepatic bile ducts in both lobes up to the peri-hilar hepatic region, with a maximum diameter of approximately 6 mm on the left and 4 mm on the right. Bile ducts at the hepatic hilum were not recognizable, nor was the common bile duct appreciated. The main hepatic duct was not dilated. Some lymph nodes were enlarged in the perihepatic region, the largest of which had diameters of approximately 8 mm × 18 mm. Signal alteration suggestive of edematous appearance of the surrounding peri-hilar adipose tissue (*Figure 7B*). These findings raised suspicion for an IMT of the liver, therefore, a cycle of steroids was stated. Aiming to further characterize the nature of the lesion, the lesion was biopsied with a percutaneous approach under US guidance using an 18 G needle. Three biopsies of the liver lesion and a bone marrow aspiration were performed. During the hospital stay, the patient underwent serial US scans and routine blood tests which showed a progressive worsening of total bilirubin levels (total bilirubin: 9.25 mg/dL). The placement of external biliary drains using a combined percutaneous and endoscopic technique was therefore deemed required. Subsequently, an anterograde cholangiography was performed with simultaneous removal of the left biliary drainage, which was found to be misplaced. This was followed by the placement of internal biliary drains using a percutaneous and endoscopic technique. The patient was then discharged in good general condition, with no more jaundice present, and total bilirubin within normal limits. However, the results of the liver biopsies proved to be inconclusive. Therefore, three more core needle biopsies of the right hepatic lobe were performed with a percutaneous approach under US guidance using an 18 G needle a couple of weeks later. Once again, the results did not provide a definitive conclusion. A CT scan was then scheduled (*Figure 7C*). It showed a hypertrophic appearance of the left hepatic lobe. In the arterial phase, large portions of the right hepatic lobe appeared hyperdense as if due to arterialization of the vascularization. On the right, the hepatic parenchyma had markedly heterogeneous density because of previous interventions and particularly due to the known poorly measurable lesion characterized by predominantly hypodense areas with irregular margins, the largest of which reaches the proximity of the hepatic hilum, especially in the right perihilar area with a central zone that is heterogeneously hyperdense as if due to vascularization. Some dilated bile ducts were appreciable on the right. The patient was then scheduled for the surgical excision of the lesion, which provided the definitive diagnosis of IMT of

the liver.

## Discussion

IMTs are rarely metastasizing neoplasms. They are characterized by a more or less dense proliferation of fibro/myofibroblastic spindle cells growing in a stroma ranging from myxoid to collagenous. Notably, these tumors exhibit a conspicuous inflammatory infiltrate, primarily composed of plasma cells and lymphocytes, with occasional eosinophils and neutrophils interspersed within (11). Preferring abdominopelvic organs and lungs of children and young adults, these lesions pose a significant challenge in differentiation from malignant tumors based solely on radiographic studies (11).

In approximately half of the IMT documented in the literature, recurrent rearrangements of the ALK gene involving the chromosome band 2p23 have been identified. These rearrangements result in the formation of a chimeric or truncated receptor tyrosine kinase with oncogenic activation and ALK kinase overexpression (3). More than 15 different genes have been identified as ALK fusion partners (TPM3, TFG, RANBP2 among others) (10). Interestingly, RANBP2-ALK fusion is associated with more aggressive clinical behaviors and unfavorable outcomes (12,13). ALK detection may hold value for differential diagnosis and planning adjuvant treatments (11). Other gene fusions affecting the tyrosine kinase pathway should be investigated in ALK-negative IMTs, including ROS1, NTRK3, and in rare cases RET or PDGFRB (14).

In general, the clinical and radiological diagnosis of IMT is often made through a process of exclusion. It is crucial to rule out infectious etiologies or more aggressive neoplasms. Therefore, these lesions are typically subjected to biopsy as the initial step in diagnosis.

One of the primary objectives of pediatric surgical oncologists is to achieve a definitive histopathological diagnosis before major surgery. Ideally, tissue biopsies should offer sufficient material for histological, immunohistochemical, molecular, and biological studies while minimizing the need for more invasive and disfiguring procedures. With advancements in surgical techniques and diagnostic capabilities, there is a growing tendency in pediatric surgical oncology to opt for endoscopic or radiologically-guided core biopsies for initial diagnosis and staging, reserving open wedge biopsies for more intricate cases (15-17). This contrasts with the initial hesitancy in the widespread use of percutaneous biopsy, stemming from the



**Table 1** Clinical manifestations and imaging examinations performed on our patients to establish a conclusive diagnosis of inflammatory myofibroblastic tumors

Variables	Case 1	Case 2	Case 3	Case 4
Age (years)	3	15	8	4
Gender	Male	Male	Male	Female
Site	Lung	Bladder	Liver	Liver
Complaining symptoms	Respiratory tract symptoms	Pelvic pain; strangury dysuria	Jaundice; pain in the right hypochondrium; acholic stools; hyperchromic urine	Vomiting diarrhea jaundice; clay-colored feces; itching
Imaging test, level I	Chest X-ray; chest US scan	Abdominal US scan	Abdominal US scan	Abdominal US scan
Imaging test, level II	Chest CT scan	Abdominal CT scan	Abdominal CT scan; MR cholangiography	Abdominal MRI
Initial biopsy	US-guided tru-cut core biopsy	Endoscopic core biopsy	Endoscopic core biopsy	Percutaneous core biopsy
Definitive biopsy	CT-guided core needle biopsy	Open biopsy	Open biopsy	Open surgery

US, ultrasound; CT, computed tomography; MR, magnetic resonance; MRI, magnetic resonance imaging.

misconception among pediatric surgeons that needle biopsy might spread tumors in children, a rare but documented risk in adults (18).

Core needle biopsies have demonstrated a high diagnostic yield for soft tissue masses, with a success rate of approximately 97%. They typically provide adequate tissue for essential ancillary testing in approximately 93% of cases (19). Furthermore, compared to open wedge biopsies, core biopsies have been demonstrated to result in lower morbidity in terms of the requirement for postoperative analgesia and blood transfusions. This often leads to reduced lengths of hospital stay for patients undergoing this type of biopsies (20).

However, when dealing with IMT in children, our research, along with other studies (21-25), has shown that core biopsies may not always be sufficient for achieving a definitive diagnosis and more precise or invasive procedures might be deemed required (*Table 1*). This is mainly due to the paucity of the material provided by the biopsy or, nevertheless, due to the diagnostic complexity and the possible differential diagnoses with a reactive process.

In accordance with our study, Dalton *et al.* (21) demonstrated that regardless of the anatomical site, only 4 out of 7 (57.1%) children with space-occupying masses had core biopsies that accurately diagnosed IMT, whereas 7 out of 8 (87.5%) incisional or excisional biopsies were successful in diagnosing IMT.

The same year, Dousek *et al.* (22) published a case

involving a 13-year-old boy who experienced long-term symptoms of dysphagia. Initially, an endoscopic biopsy failed to provide a definitive diagnosis. Subsequently, the patient required an open biopsy via a right-sided posterolateral thoracotomy to ultimately establish the definitive diagnosis of IMT. Similarly, in 2019, Thavamani *et al.* (23) reported the case of a 10-year-old girl who presented with portal hypertension due to a mass in the porta hepatis. Although the endoscopic core biopsy initially revealed benign hyperplastic lymphoid tissue, it was ultimately the open liver biopsy performed with laparotomy access that established the definitive diagnosis of IMT of the liver. More recently, Sahraie *et al.* (24) reported the case of a 5-year-old girl with a space-occupying lesion in the head of the pancreas. Multiple reviews of the CT-guided core needle biopsy specimen were required to raise suspicion of IMT, which was subsequently confirmed upon examination of the resected specimen obtained from the Whipple procedure. Similarly, Morales Prillwitz *et al.* (25) required an exploratory laparotomy to ascertain the etiology of an abdominal mass located between the spleen and the liver. Subsequent histopathological examination revealed it to be an IMT of the stomach.

The inconclusive results obtained from core biopsies in cases of IMT may stem from various factors. These may include the absence of standardized technical protocols and indications regarding the optimal needle size, or the number of cores required. However, it is more likely that

these inconclusive results are primarily due to the limited amount of tissue obtained, which may not be sufficient for performing all the necessary tests to reach a definitive diagnosis, such as histopathology, IHC, and genetic analysis. Additional factors depend on the experience of the operator and the need for a learning curve for performing these minimally invasive procedures. Moreover, the diagnostic complexity and possible differential diagnoses with reactive processes require pathologists specialized in this field of expertise, usually working in tertiary referral centers.

In conclusion, while acknowledging the limitations of primarily isolated case reports and small series in the literature, the main clinical, laboratory, and radiological features of IMT often remain nonspecific. Our study, along with others (21-25), suggests that when these neoplasms are suspected in children, more precise procedures are warranted to achieve a definitive diagnosis and eventually initiate targeted treatments with tyrosine kinase inhibitors.

## Conclusions

Despite core biopsies being typically sufficient for definitively diagnosing most solid tumors in children, our study and others have shown that they can yield inconclusive results in the case of IMT. When faced with clinically and radiologically suspected IMT in children, our findings suggest that more precise procedures might be required to achieve a definitive diagnosis.

## Acknowledgments

We would like to thank the Foundation Romeo and Enrica Invernizzi for supporting this project. Moreover, we would like to acknowledge the support of the APC central fund of the University of Milano.

*Funding:* None.

## Footnote

*Reporting Checklist:* The authors have completed the AME Case Series reporting checklist. Available at <https://tp.amegroups.com/article/view/10.21037/tp-24-239/rc>

*Peer Review File:* Available at <https://tp.amegroups.com/article/view/10.21037/tp-24-239/prf>

*Conflicts of Interest:* All authors have completed the ICMJE uniform disclosure form (available at <https://tp.amegroups.com/article/view/10.21037/tp-24-239/coif>). The authors have no conflicts of interest to declare.

*Ethical Statement:* The authors are accountable for all aspects of the work in ensuring that questions related to the accuracy or integrity of any part of the work are appropriately investigated and resolved. All procedures performed in this study were in accordance with the ethical standards of the institutional and/or national research committee(s) and with the Helsinki Declaration (as revised in 2013). According to our Institution's regulations (Department of Pediatric Surgery, Children's Hospital "Vittore Buzzi", Milan, Italy), the need for ethical approval for this non-interventional study's retrospectively obtained and anonymized data was waived. The reservedness of the collected information was ensured according to Regulation (EU)/2016/679 GDPR [Regulation (EU) 2016/679], Legislative Decree n.101/18. Full informed consent was obtained from the study participants' guardians.

*Open Access Statement:* This is an Open Access article distributed in accordance with the Creative Commons Attribution-NonCommercial-NoDerivs 4.0 International License (CC BY-NC-ND 4.0), which permits the non-commercial replication and distribution of the article with the strict proviso that no changes or edits are made and the original work is properly cited (including links to both the formal publication through the relevant DOI and the license). See: <https://creativecommons.org/licenses/by-nc-nd/4.0/>.

## References

1. Fletcher CD. The evolving classification of soft tissue tumours: an update based on the new WHO classification. *Histopathology* 2006;48:3-12.
2. Casanova M, Brennan B, Alaggio R, et al. Inflammatory myofibroblastic tumor: The experience of the European pediatric Soft Tissue Sarcoma Study Group (EpSSG). *Eur J Cancer* 2020;127:123-9.
3. Centre international de recherche sur le cancer, Organisation mondiale de la santé, eds. *Paediatric Tumours*. 5th ed. International agency for research on cancer; 2022.
4. Hammas N, Chbani L, Rami M, et al. A rare tumor of the lung: inflammatory myofibroblastic tumor. *Diagn Pathol* 2012;7:83.
5. Karnak I, Senocak ME, Ciftci AO, et al. Inflammatory myofibroblastic tumor in children: diagnosis and

- treatment. *J Pediatr Surg* 2001;36:908-12.
6. Pire A, Orbach D, Galmiche L, et al. Clinical, pathologic, and molecular features of inflammatory myofibroblastic tumors in children and adolescents. *Pediatr Blood Cancer* 2022;69:e29460.
  7. Arredondo Montero J, Pérez Riveros BP, Bronte Anaut M, et al. Ileal Inflammatory Myofibroblastic Tumor in a Two-Month-Old Girl: Long-Term Follow-up. *Indian J Pediatr* 2022;89:1264.
  8. Jang EJ, Kim KW, Kang SH, et al. Inflammatory myofibroblastic tumors arising from pancreas head and peri-splenic area mimicking a malignancy. *Ann Hepatobiliary Pancreat Surg* 2021;25:287-92.
  9. Mahajan P, Casanova M, Ferrari A, et al. Inflammatory myofibroblastic tumor: molecular landscape, targeted therapeutics, and remaining challenges. *Curr Probl Cancer* 2021;45:100768.
  10. Sommer S, Schmutz M, Schaller T, et al. Individualized targeted treatment in a case of a rare TFG::ROS1 fusion positive inflammatory myofibroblastic tumor (IMT). *Cancer Rep (Hoboken)* 2024;7:e1916.
  11. Lopez-Nunez O, John I, Panasiti RN, et al. Infantile inflammatory myofibroblastic tumors: clinicopathological and molecular characterization of 12 cases. *Mod Pathol* 2020;33:576-90.
  12. Antonescu CR, Suurmeijer AJ, Zhang L, et al. Molecular characterization of inflammatory myofibroblastic tumors with frequent ALK and ROS1 gene fusions and rare novel RET rearrangement. *Am J Surg Pathol* 2015;39:957-67.
  13. Chen ST, Lee JC. An inflammatory myofibroblastic tumor in liver with ALK and RANBP2 gene rearrangement: combination of distinct morphologic, immunohistochemical, and genetic features. *Hum Pathol* 2008;39:1854-8.
  14. Baldi GG, Brahmi M, Lo Vullo S, et al. The Activity of Chemotherapy in Inflammatory Myofibroblastic Tumors: A Multicenter, European Retrospective Case Series Analysis. *Oncologist* 2020;25:e1777-84.
  15. Deeney S, Stewart C, Treece AL, et al. Diagnostic utility of core needle biopsy versus open wedge biopsy for pediatric intraabdominal solid tumors: Results of a prospective clinical study. *J Pediatr Surg* 2017;52:2042-6.
  16. Malkan AD, Loh AH, Sandoval JA. Minimally invasive surgery in the management of abdominal tumors in children. *J Pediatr Surg* 2014;49:1171-6.
  17. Pohlig F, Kirchhoff C, Lenze U, et al. Percutaneous core needle biopsy versus open biopsy in diagnostics of bone and soft tissue sarcoma: a retrospective study. *Eur J Med Res* 2012;17:29.
  18. Garrett KM, Fuller CE, Santana VM, et al. Percutaneous biopsy of pediatric solid tumors. *Cancer* 2005;104:644-52.
  19. Metz T, Heider A, Vellody R, et al. Image-guided percutaneous core needle biopsy of soft-tissue masses in the pediatric population. *Pediatr Radiol* 2016;46:1173-8.
  20. Overman RE, Kartal TT, Cunningham AJ, et al. Optimization of percutaneous biopsy for diagnosis and pretreatment risk assessment of neuroblastoma. *Pediatr Blood Cancer* 2020;67:e28153.
  21. Dalton BG, Thomas PG, Sharp NE, et al. Inflammatory myofibroblastic tumors in children. *J Pediatr Surg* 2016;51:541-4.
  22. Dousek R, Tuma J, Planka L, et al. Inflammatory myofibroblastic tumor of the esophagus in childhood: a case report and a review of the literature. *J Pediatr Hematol Oncol* 2015;37:e121-4.
  23. Thavamani A, Mandelia C, Anderson PM, et al. Pediatric Inflammatory Myofibroblastic Tumor of the Liver: A Rare Cause of Portal Hypertension. *ACG Case Rep J* 2019;6:1-4.
  24. Sahraie R, Kashanizadeh A, Zamani F, et al. Inflammatory myofibroblastic tumor of head of pancreas in a 5 Year-Old child. *Journal of Pediatric Surgery Case Reports* 2021;69:101856.
  25. Morales Prillwitz O, Pérez Hurtado B, Olaya Álvarez S, et al. Gastric inflammatory myofibroblastic tumor in a 10-month-old girl: A case report. *Int J Surg Case Rep* 2020;68:185-9.

**Cite this article as:** Pierucci UM, Paraboschi I, Ardenghi C, Viglio C, Selvaggio GGO, Lanfranchi G, Casanova M, Collini P, Barisella M, Napolitano M, Camporesi A, Pelizzo G. Efficacy of core biopsies for diagnosing inflammatory myofibroblastic tumors in pediatric patients: case series from a single tertiary referral center. *Transl Pediatr* 2024;13(10):1799-1809. doi: 10.21037/tp-24-239